

# The gut microbiota and metabolome is associated with diminished COVID-19 vaccine-induced antibody responses in immunosuppressed inflammatory bowel disease patients

James L Alexander (✉ [j.alexander@imperial.ac.uk](mailto:j.alexander@imperial.ac.uk))

Imperial College London

Benjamin H Mullish

Nathan P Danckert

Zhigang Liu

Aamir Saifuddin

Melissa Torkizadeh

Hajir Ibraheim

Jesús Miguéns Blanco

Lauren A Roberts

Claire M Bewshea

Rachel Nice

Simeng Lin

Hemanth Prabhudev

Caroline Sands

Verena Horneffer-van der Sluis

Matthew Lewis

Shaji Sebastian

Charlie W. Lees

Julian P Teare

Ailsa Hart

James R. Goodhand

Nicholas A. Kennedy

Julian R. Marchesi

Tariq Ahmad

Nick Powell (✉ [npowell@ic.ac.uk](mailto:npowell@ic.ac.uk))

Imperial College London

**Keywords:** Gut microbiota, Metabolome, SARS-CoV-2, inflammatory bowel disease, anti-TNF therapy, infliximab, vaccine, ChAdOx1 nCoV-19, BNT162b2

**Posted Date:** May 23rd, 2022

**DOI:** <https://doi.org/10.21203/rs.3.rs-1672833/v1>

**License:**  This work is licensed under a Creative Commons Attribution 4.0 International License.

[Read Full License](#)

---

**Version of Record:** A version of this preprint was published at EBioMedicine on January 10th, 2023. See the published version at <https://doi.org/10.1016/j.ebiom.2022.104430>.

# Abstract

Patients with inflammatory bowel disease (IBD) treated with anti-TNF therapy exhibit attenuated humoral immune responses to vaccination against SARS-CoV-2. The gut microbiota and its functional metabolic output, which are perturbed in IBD, play an important role in shaping host immune responses. We explored whether the gut microbiota and metabolome could explain variation in anti-SARS-CoV-2 vaccination responses in immunosuppressed IBD patients.

Faecal and serum samples were prospectively collected from infliximab-treated patients with IBD in the CLARITY-IBD study undergoing vaccination against SARS-CoV-2. Antibody responses were measured following two doses of either ChAdOx1 nCoV-19 or BNT162b2 vaccine. Patients were classified as having responses above or below the geometric mean of the wider CLARITY-IBD cohort. 16S rRNA gene amplicon sequencing, nuclear magnetic resonance (NMR) spectroscopy and bile acid profiling with ultra-high-performance liquid chromatography mass spectrometry (UHPLC-MS) were performed on faecal samples. Univariate, multivariable and correlation analyses were performed to determine gut microbial and metabolomic predictors of response to vaccination.

Forty-three infliximab-treated patients with IBD were recruited (30 Crohn's disease, 12 ulcerative colitis, 1 IBD-unclassified; 26 with concomitant thiopurine therapy). Eight patients had evidence of prior SARS-CoV-2 infection. Seventeen patients (39.5%) had a serological response below the geometric mean. Gut microbiota diversity was lower in below average responders ( $p = 0.021$ ). *Bifidobacteria* abundance was associated with better serological response, while *Streptococcus* was associated with poorer response. The faecal metabolome was distinct between above and below average responders (OPLS-DA  $R^2X$  0.25,  $R^2Y$  0.26,  $Q^2$  0.15; CV-ANOVA  $p = 0.038$ ). Trimethylamine was associated with better response, while succinate, phenylalanine and the bile acids tauroolithocholate and taurodeoxycholate were associated with poorer response.

Our data suggest that there is an association between the gut microbiota and variable serological response to vaccination against SARS-CoV-2 in immunocompromised patients. Microbial metabolites including trimethylamine may be important in mitigating anti-TNF-induced attenuation of the immune response.

## Introduction

Vaccination against SARS-CoV-2 is an effective strategy to limit infections, hospitalisations and deaths caused by COVID-19.<sup>1,2</sup> However, SARS-CoV-2 vaccine immunogenicity is diminished in some immunosuppressed groups. Patients with inflammatory bowel disease (IBD) treated with anti-TNF therapy have attenuated serological responses to vaccination against SARS-CoV-2, which is associated with increased risk of breakthrough infection<sup>3-5</sup>. However, even in anti-TNF recipients, vaccine-induced antibody responses are highly heterogeneous. Such variability is not explained by known modifiers of

vaccine response including age, vaccine type or concomitant immunomodulator use,<sup>3</sup> indicating that other, undefined factors influence vaccine immunogenicity.

The gut microbiota is critical in shaping host immune responses, and microbiota function has been proposed as a potential modulator of response to vaccination. In infants, faecal microbiota composition is associated with responses to oral rotavirus vaccines.<sup>6,7</sup> In adults given a broad-spectrum antibiotic intervention prior to vaccination against influenza,<sup>8</sup> reduced H1N1-specific neutralization and IgG1 and IgA binding antibody titres were observed. Lower titres were correlated with both bacterial and metabolomic phenotypes and, in particular, a 1000-fold reduction in serum secondary bile acids. Impaired antibody responses to influenza vaccine have been shown in antibiotic-treated, germ-free and *Tlr5*<sup>-/-</sup> mice compared to littermate controls.<sup>9</sup> Such an effect was also seen with inactivated poliovirus, but not with other vaccines against Hepatitis B and yellow fever.<sup>9</sup> The ability of faecal microbiota transplant to rescue impaired immune responses to several vaccines has also been demonstrated in preclinical models.<sup>10</sup> A recent study of recipients of SARS-CoV-2 vaccination has shown associations between gut microbiota composition and neutralising antibody responses in a group of non-immunosuppressed healthy volunteers.<sup>11</sup>

Inflammatory bowel disease is associated with perturbation of gut microbiota composition and function.<sup>12,13</sup> Microbiota composition has also been linked to therapeutic responses to immunosuppressive therapies in IBD,<sup>14</sup> and gut microbial metabolites are predictive of response to anti-TNF therapy.<sup>15,16</sup> Given the three-way interaction between IBD, the gut microbiota and immunosuppressive therapy, we conducted a prospective observational study to explore the hypothesis that gut microbiota composition and function influence immune response to SARS-CoV-2 vaccination in immunosuppressed patients with IBD.

## Results

Forty-three patients with IBD were recruited between 25th January and 15th March 2021. Demographics are shown in Table 1.

Table 1  
Participant characteristics (total n = 43)

Characteristics	N (%)
Male:Female	27:16
Median age (range)	40 (19–67)
Vaccine:	15
<i>Oxford/AstraZeneca</i>	28
<i>Pfizer/BioNTech</i>	
IBD therapy:	43 (100%)
<i>Infliximab</i>	26 (60.5%)
<i>Thiopurine</i>	
IBD subtype:	30
<i>Crohn's disease</i>	12
<i>Ulcerative colitis</i>	1
<i>IBD-unclassified</i>	
Prior SARS-CoV-2 infection	8 (18.6%)
Median faecal calprotectin (IQR)	196 (56–485)

## Anti-SARS-CoV-2 (S) antibody level following two doses of COVID-19 vaccine

Anti-SARS-CoV-2 spike antibodies were measured between 14 and 100 days after the second dose of vaccination (Fig. 1b). Across the cohort, 25 patients (58.1%) had antibody levels above the geometric mean, specific to their vaccine type and prior infection status; 18 patients (41.9%) had antibody levels below the geometric mean. There were no significant differences in the proportions of patients above and below the geometric mean when stratified by age, IBD subtype, vaccine type, immunomodulator use or patient gender (supplementary Figs. 1a-e).

## Gut microbiota composition is associated with response to anti-SARS-CoV-2 vaccination

Baseline gut microbiota composition was found to differ between vaccine recipients with above average antibody concentrations compared to those with below average concentrations. Although there were no differences in Chao1 or Shannon alpha diversity metrics between the groups (Fig. 2a,b), nor on Permutational multivariate analysis of variance (PERMANOVA), beta diversity analysis demonstrated reduced dispersion of inter-sample Aitchison distances in the below average group compared to the

above average group (Fig. 2c; Permutation Test for Constrained Correspondence Analysis, Redundancy Analysis and Constrained Analysis of Principal Coordinates  $p = 0.021$ ). The dominant phyla in above and below average responders to both the BNT162b2 and the ChAdOx1 nCoV-19 vaccines were *Bacteroidota* and *Firmicutes* (Fig. 2d). The proportion of *Bacteroidota* was lower in below average responders to both vaccines, although this was not statistically significant (Fig. 2d). After accounting for covariates including IBD subtype, vaccine type, immunomodulator use, patient age and gender, a total of seven ASVs were differentially abundant between above and below average responders (Fig. 2e). In particular, *Bilophila*, was associated with above average response (coefficient 1.23 [95% CI 0.05–2.40]), and *Streptococcus*, was predictive of below average response (-1.39 [-2.35 - -0.59]).

## Gut metabolome is associated with response to anti-SARS-CoV-2 vaccination

<sup>1</sup>H-NMR profiles were first used to interrogate global metabolite profiles in above and below average responders. In multivariate analysis, the faecal metabolome of above average responders to vaccination was distinct from that of below average responders (Fig. 3a; PCA  $R^2X$  0.42,  $Q^2$  0.12; OPLS-DA model  $R^2X$  0.25,  $R^2Y$  0.26,  $Q^2$  0.15, CV-ANOVA  $p = 0.038$ ). A total of 36 metabolite features were identified from <sup>1</sup>H-NMR, including five short chain fatty acids, eleven amino acids and three respiratory compounds. 50 bile acids were assigned with targeted UHPLC-MS. In univariate analysis (Fig. 3b-d), higher levels of trimethylamine (coefficient 0.10 [95% CI 0.02–0.17]), omega-muricholic acid (0.89 [0.35–1.43]) and ursodeoxycholic acid (0.60 [0.10–1.11]) were found in the faecal metabolomes of patients with above average responses to vaccination. Below average vaccine response was characterised by abundance of succinate (coefficient - 5.65, [95% CI -1.14 - -10.16]), phenylalanine (-0.71 [-1.09 - -0.34]) and phenylacetate (-5.60 [-10.07 - -1.12]). The bile acids tauroolithocholate (coefficient - 0.50 [95% CI -0.81 - -0.20]) and taurodeoxycholate (-0.61 [-1.04 - -0.17]) were also present at higher levels in below average responders.

## Integration of microbiome and metabolite data

Finally, correlation analysis was performed to determine metabolites that were associated with significant ASVs. *Streptococcus* was positively correlated with the amino acid phenylalanine ( $r = 0.25$ ); both were associated with below average response to vaccination in earlier independent analysis. *Streptococcus* was also correlated with taurocholic acid ( $r = 0.31$ ), taurohyocholic acid ( $r = 0.32$ ) and tauro-omega-muricholic acid ( $r = 0.26$ ). *Bilophila* was positively associated with methylamine and trimethylamine ( $r = 0.37$  &  $0.23$  respectively), and chenodeoxycholic acid ( $r = 0.22$ ). *Dialister* was positively correlated with several amino acids – alanine ( $r = 0.25$ ), isoleucine ( $r = 0.31$ ) and methionine ( $r = 0.30$ ). The short chain fatty acid acetate was negatively correlated with *Streptococcus* ( $r = -0.22$ ), while valerate was negatively correlated with *Bilophila* ( $r = -0.30$ ).

## Discussion

To our knowledge, this study is the first to demonstrate a link between the metabolic function of the gut microbiota and immune responses to SARS-CoV-2 vaccination. These findings are particularly important because they pertain to an immunosuppressed group known to have diminished immunogenicity to vaccination, in whom rates of breakthrough SARS-CoV-2 infection are increased.

There is growing evidence from human<sup>8</sup> and animal studies<sup>9,10</sup> that the gut microbiota plays a role in modulating immune responses to vaccination, and the baseline composition of the gut microbiota has recently been shown to predict serological response to COVID-19 vaccines.<sup>11</sup> There are a number of important differences between our study and that of Ng and colleagues, in which the majority of participants received CoronaVac, which is an inactivated virus vaccine, and a minority received BNT162b2 (mRNA vaccine). In our study the majority of participants received BNT162b2 and a minority received ChAdOx1 nCoV-19 (adenovirus vector vaccine). The two studies were carried out in different countries (Hong Kong and United Kingdom). Perhaps most importantly all participants in our study had IBD and were on infliximab, whereas the Ng study included predominantly healthy individuals, with fewer than 3% on any form of immunosuppressive therapy. Despite these differences, a common finding in both studies was that a *Parabacteroides* was associated with lower serological response to vaccination.

In our study *Bilophila* genus abundance was associated with higher serological response to SARS-CoV-2 vaccination. Elevated *Bilophila* abundance has been reported in treatment-naïve IBD patients<sup>17</sup> and *Bilophila wadsworthensis* is associated with an enhanced pro-inflammatory T<sub>H</sub>1 response and development of colitis in *Il10*<sup>-/-</sup> mice.<sup>18</sup> Notably, vaccination with BNT162b2 leads to induction of virus-specific CD4 + T cell responses with a T<sub>H</sub>1 profile.<sup>19,20</sup> It might be postulated that *Bilophila* is acting as a vaccine adjuvant in some IBD patients, engaging beneficial T-cell help to support the generation of antibodies against SARS-CoV-2.

Our data suggest that the gut microbiota derived metabolite trimethylamine (TMA) may be acting to ameliorate the attenuated vaccine-induced immune response seen in anti-TNF recipients. TMA is a breakdown product of gut microbial metabolism of the dietary constituents choline and carnitine.<sup>21</sup> TMA is metabolised in the liver to trimethylamine N-oxide (TMAO), high plasma levels of which have been linked to the development of cardiovascular disease.<sup>22</sup> Interestingly, the notion of TMAO as an immune sensitiser has recently been disclosed through its enhancement of the efficacy of cancer immunotherapy via promotion of CD8<sup>+</sup> T cell-mediated immunity.<sup>23</sup>

We found several faecal metabolites, including phenylalanine, phenylacetate and succinate, which are associated with reduced vaccine-induced serological responses. Faecal phenylalanine has been found at higher levels in IBD patients compared to healthy controls.<sup>24-26</sup> Its metabolism has also been linked to the immune response to the bacillus Calmette-Guérin (BCG) vaccine.<sup>27</sup> Succinate is found at higher levels in the gut of patients with ulcerative colitis relative to healthy controls.<sup>28,29</sup> Succinate is also up-regulated in patients with fistulising Crohn's disease and is implicated in the epithelial to mesenchymal transition

process.<sup>30</sup> Paradoxically, succinate has also been shown to have anti-inflammatory activity via tuft cells in the small intestine.<sup>31</sup>

We recognise several limitations in our study. Although our results are significant after correction for multiple testing, the relatively small cohort means that the findings would benefit from validation in larger populations. In our analysis we have accounted for confounding factors including age, gender, IBD subtype and IBD therapy, but we were not able to account for other factors known to influence the gut microbiome and metabolome such as diet. We have focussed our metabolomic analysis on faecal samples, and future studies of a broader analysis of other biofluids including blood would be interesting. Furthermore, our immunological analysis is restricted to humoral immunity, and without T cell response data we are unable to draw conclusions on how the microbiota interact with vaccine-induced cell-mediated immunity.

In conclusion, these results suggest a possible link between the composition and function of the gut microbiota and impaired serological response to SARS-CoV-2 vaccination. These data imply that therapeutics targeted at modulating the microbiota, or even supplementation of beneficial metabolites, might be effective strategies to ameliorate diminished vaccine-induced immunogenicity in vulnerable groups.

## Patients And Methods

### Recruitment and sampling

Patients with IBD established on infliximab treatment for greater than 12 weeks were recruited at two centres (Imperial College Healthcare NHS Trust and London North West University Healthcare NHS Trust). All participants were in the CLARITY-IBD study (<https://www.clarityibd.org/>),  $\geq 18$  years old and undergoing vaccination against SARS-CoV-2. Participants were excluded at screening if they had received antibiotics within 6 weeks of recruitment. All recruited subjects provided written informed consent.

Faecal and blood samples were collected from patients either when they attended hospital infusion units to receive infliximab, or on the day they attended the hospital vaccine centre to receive their first dose of anti-SARS-CoV-2 vaccine. The majority of faecal samples were collected shortly before the first dose of vaccine was given and 81% of faecal samples were collected within 4 weeks of the first dose. Blood samples were collected at 8-week intervals according to the CLARITY-IBD study protocol (available at <https://www.clarityibd.org/>).

Whole faeces were collected in a faeces collector (FECOTAINER®, AT Medical BV, The Netherlands). Fresh faecal samples were transferred to the laboratory within six hours of collection, homogenized and aliquoted for storage at  $-80^{\circ}\text{C}$  pending analysis. An experimental schema is shown in Fig. 1a.

### Anti-SARS-CoV2 Serology:

Anti-SARS-CoV-2 serology laboratory analyses were performed at the Academic Department of Blood Sciences at the Royal Devon and Exeter NHS Foundation Trust. To determine antibody responses specific to vaccination we used the Roche Elecsys Anti-SARS-CoV-2 spike (S) electrochemiluminescence immunoassay.<sup>32</sup> This double sandwich electrochemiluminescence immunoassay uses a recombinant protein of the receptor binding domain (RBD) on the spike protein as an antigen for the determination of antibodies against SARS-CoV-2. Sample electrochemiluminescence signals are compared with an internal calibration curve and quantitative values are reported as units (U)/mL. In-house validation experiments have been described previously.<sup>3</sup>

All participants were tested for previous SARS-CoV-2 infection using the Roche Elecsys anti-SARS-CoV-2 (N) immunoassay. A concentration of greater than or equal to 0.12 U/ml was defined as a threshold below which participants were deemed to have no evidence of prior infection. Participants who reported a previous PCR test confirming SARS-CoV-2 infection at any time prior to vaccination were deemed to have evidence of past infection irrespective of any antibody test result.

All participants in the study had serological analyses at 8-week intervals, irrespective of when their vaccine doses were given. To standardise our analysis, we took the anti-S RBD antibody concentration at the first time-point measured post-second vaccine dose (but no earlier than 14 days after the second dose). This concentration was compared to the geometric mean at the relevant time point as measured in the infliximab-treated CLARITY-IBD cohort (specific to vaccine-type and presence/absence of prior natural infection). Participants were classified as having serological responses above or below their vaccine-type, infection-specific geometric mean.

## **16S rRNA gene sequencing:**

DNA was extracted from crude faecal samples using the DNeasy PowerLyzer PowerSoil Kit (Qiagen, Hilden, Germany) following manufacturer's instruction with the modification that samples were homogenized in a Bullet Blender Storm bead beater (Cambio, St Albans, UK). DNA was quantified using a Qubit Fluorometer (ThermoFischer, UK), and was aliquoted and stored at -80°C until ready for downstream use. Sample libraries were prepared following Illumina's 16S Metagenomic Sequencing Library Preparation Protocol<sup>33</sup> using specifically designed V1/V2 hypervariable region primers<sup>34</sup>. Pooled sample library sequencing was performed using the Illumina MiSeq platform (Illumina Inc, Saffron Walden, UK) and the MiSeq Reagent Kit v3 (Illumina) using paired-end 300-bp chemistry. Processing of sequencing data was performed via the DADA2 pipeline (v1.18) as previously described<sup>35</sup>, using the SILVA bacterial database Version 138.1 (<https://www.arb-silva.de/> (accessed on 08/10/2021)). Pre-processed assigned sequence variants (ASVs) data were further cleaned and filtered using the decontam pipeline removing contaminating DNA features.<sup>36</sup>

## **Metabolomic profiling using <sup>1</sup>H-NMR:**

Faecal metabolite extraction was performed as previously published with modification.<sup>37</sup> 600 mg of each faecal sample was mixed with 1200 µl water, vortexed for 5 min and spun at 20,000 g for 10 min at 4°C.

540  $\mu$ l supernatants were collected and mixed with 60  $\mu$ l phosphate buffer containing 1.5 M  $\text{KH}_2\text{PO}_4$ , 1 mM  $\text{NaN}_3$  and 1‰ TSP. 570  $\mu$ l of the mixtures were transferred into a 5 mm NMR tube for analysis. One-dimensional proton NMR spectra was acquired using a Bruker 600 MHz spectrometer (Bruker, Rheinstetten, Germany) at 300 K employing a standard NOESY pulse sequence (relaxation delay – 90° - t1 – 90° - tm – 90° - acquisition). Relaxation delay was set to 4 s, while t1 and tm were set to 4  $\mu$ s and 100 ms, respectively. 32 scans were performed into 64 K data points with a spectral width of 20 ppm. Fourier transformation, phase and baseline correction and calibration of TSP at  $\delta$  0.0 of NMR spectral were carried out in Topspin V3.0 software (Bruker Biospin). Data were imported into MATLAB R2014a (MathWorks Inc., Natick, USA) with a resolution of 0.0005 ppm for further processing. After the removal of the water peak ( $\delta$  4.7–4.9) and TSP peak ( $\delta$  -1–0.6), the spectra were automatically aligned using the recursive segment-wise peak alignment (RSPA) alignment algorithm to reduce peak shifting affects,<sup>38</sup> and also normalized by the probabilistic quotient method to diminish inter-sample concentration variability.<sup>39</sup> Metabolites were assigned using Chenomx NMR Suite 8.31 (Chenomx Inc., Edmonton, Canada) and published literature.<sup>37</sup> Statistical Total Correlation Spectroscopy (STOCSY) analysis was employed to assist the metabolite identification.<sup>40</sup>

## Bile acid profiling using UHPLC-MS

Faecal samples were analysed using ultra high-performance liquid chromatography-mass spectrometry (UHPLC-MS) for the profiling of bile acids. The protocols used for faecal extract preparation and sample acquisition were as previously described<sup>34,41,42</sup>. In brief, 75  $\mu$ L aliquots were taken from each sample and diluted 1:3 v/v with water including a mixture of stable isotope-labelled internal standards added in order to monitor data quality during acquisition. To assess retention time drift (and for subsequent bile acid annotation) mixes of bile acid standard references were also acquired as part of the analysis run. For quality control (QC) and pre-processing, a pooled QC sample was prepared by combining equal parts of each study sample and acquired regular intervals during sample analyses. An additional set of QC sample dilutions was created and analysed at the start and end of sample analyses for assessment of analyte response.<sup>43</sup>

Sample analysis was performed on an ACQUITY UPLC instrument (Waters Corp., Milford, MA, USA) coupled to Xevo G2-S Q-TOF mass spectrometers (Waters Corp., Manchester, UK) via a Z-spray electrospray ionisation (ESI) source operating in both negative ion mode. In addition, to increase certainty in bile acid metabolite annotation, this data was analyzed using peakPanther, an automated pipeline for the detection, integration and reporting of predefined metabolites from LC-MS data<sup>44</sup>. Datasets were pre-processed using the nPYc-Toolbox.<sup>45</sup> Pre-processing included elimination of potential run-order effects and feature filtering to retain only features/metabolites measured with a high analytical quality (relative standard deviation, RSD in pooled QC < 30%, pooled QC dilution series Pearson correlation to dilution factor > 0.7, RSD in study samples > 1.1\* RSD in pooled QC). Using these techniques, the relative abundances of 50 bile acid species were obtained.

## Statistical analysis

A combination of R packages was used to analyse and visualise faecal microbiota sequencing data, including Phyloseq<sup>46</sup>, Vegan<sup>47</sup>, and ggplot2<sup>48</sup>. To assess feature changes in alpha-diversity, mixed effects models<sup>49</sup> compared Shannon's diversity index and Chao1 richness and with the average antibody concentration (i.e. above or below geometric mean, categorical) adjusting for covariates (age, vaccine-type, IBD subtype, immunomodulator use and gender). Aitchison distance was used for beta-diversity analyses<sup>50</sup> after centre log-ratio data transformation (CLR)<sup>51</sup>; principal coordinates analyses (PCoA) were generated to visualise the (dis)similarity between groups. Permutational multivariate analysis of variance (PERMANOVA) and Permutation Test for Constrained Correspondence Analysis, Redundancy Analysis and Constrained Analysis of Principal Coordinates were used to statistically compare groupings within the data<sup>47</sup>. Differential abundance analysis of ASVs was calculated using ANCOM-BC<sup>52</sup> with Holm-Bonferroni p-value correction and a mixed effects model (adjusting for aforementioned covariates) with false discovery rate (FDR) correction.<sup>49</sup>

1H-NMR and UHPLC-MS data were analysed using SIMCA (v17) and R (v4.0.3). After Pareto scaling of 1H-NMR data, unsupervised Principal Components Analysis (PCA) and supervised Orthogonal Projections to Latent Structures Discriminant Analysis (OPLS-DA) were performed with further interrogation of data using S plot and validation of supervised models using CV-ANOVA. Mixed effects models<sup>53</sup> assessed metabolite differences between groups with differentially abundant metabolites reported with q value < 0.2 after correction for multiple testing (Benjamini-Hochberg false discovery rate). Finally, Spearman correlation of statistically significant ASVs with metabolites was performed using corrplot (q < 0.2 considered significant after false discovery rate p value correction).

## Ethical consideration and role of funders

Human samples used in this research project were obtained from the Imperial College Healthcare Tissue Bank (ICHTB). ICHTB is supported by the National Institute for Health Research (NIHR) Biomedical Research Centre based at Imperial College Healthcare NHS Trust and Imperial College London. ICHTB is approved by Wales REC3 to release human material for research (17/WA/0161). All participants were co-recruited from the CLARITY-IBD study (20/HRA/3114).

## Declarations

### *Ethical consideration and role of funders*

Human samples used in this research project were obtained from the Imperial College Healthcare Tissue Bank (ICHTB). ICHTB is supported by the National Institute for Health Research (NIHR) Biomedical Research Centre based at Imperial College Healthcare NHS Trust and Imperial College London. ICHTB is approved by Wales REC3 to release human material for research (17/WA/0161). All participants were co-recruited from the CLARITY-IBD study (20/HRA/3114).

**Acknowledgements:** JLA is the recipient of an NIHR Academic Clinical Lectureship (CL-2019-21-502), funded by Imperial College London and The Joyce and Norman Freed Charitable Trust. BHM is the

recipient of an NIHR Academic Clinical Lectureship (CL-2019-21-002). The Division of Digestive Diseases at Imperial College London receives financial and infrastructure support from the NIHR Imperial Biomedical Research Centre (BRC) based at Imperial College Healthcare NHS Trust and Imperial College London. Metabolomics studies were performed at the MRC-NIHR National Phenome Centre at Imperial College London; this centre receives financial support from the Medical Research Council (MRC), the National Institute of Health Research (NIHR) (grant number MC\_PC\_12025) and infrastructure support from the NIHR Imperial Biomedical Research Centre (BRC). The NIHR Exeter Clinical Research Facility is a partnership between the University of Exeter Medical School College of Medicine and Health, and Royal Devon and Exeter NHS Foundation Trust. This project is supported by the National Institute for Health Research (NIHR) Exeter Clinical Research Facility. The views expressed are those of the authors and not necessarily those of the NIHR or the Department of Health and Social Care.

**Data Availability:** Sequencing data from this study (in fastq-format) are publicly available for download at the European Nucleotide Archive (ENA) database using study accession number PRJEB52928 (<http://www.ebi.ac.uk/ena/data/view/PRJEB52928>). The datasets used and/or analysed during the current study are available from the corresponding author on reasonable request.

**Author contributions:** JLA, BHM, TA and NP designed the study; JLA, AS, HP and MT collected the samples. JLA, NPD and JMB undertook microbiome analysis; JLA, ZL, BHM, VH and CS undertook metabolomic analysis. JLA, BHM, NPD, ZL and NP wrote the first draft of the manuscript. All authors contributed to writing of and approved the final manuscript.

#### **Disclosure statement:**

Dr Alexander reports sponsorship from Vifor Pharma for accommodation/travel, outside the submitted work. Dr Saifuddin has received travel expense support from Janssen. Dr. Kennedy reports grants from AbbVie, Biogen, Celgene, Celtrion, Galapagos, MSD, Napp, Pfizer, Pharmacosmos, Roche and Takeda, consulting fees from Amgen, Bristol-Myers Squibb, Falk, Janssen, Mylan, Pharmacosmos, Galapagos, Takeda and Tillotts, personal fees from Allergan, Celltrion, Falk, Ferring, Janssen, Pharmacosmos, Takeda, Tillotts, Galapagos, and support for attending meetings from AbbVie, Falk and Janssen outside the submitted work. Prof. Sebastian reports grants from Takeda, Abbvie, Tillots Pharma, Janssen, Pfizer, Biogen and personal fees from Takeda, Abbvie, Janssen, Pharmacosmos, Biogen, Pfizer, Tillots Pharma and Falk Pharma, outside the submitted work. Dr Hart reports payment or honoraria for lectures, presentations, speakers bureaus, manuscript writing or educational events from AbbVie, AZ, Atlantic, Bristol-Myers Squibb, Celltrion, Falk, Galapagos, Janssen, MSD, Napp Pharmaceuticals, Pfizer, Pharmacosmos, Shire and Takeda and Global Steering Committee for Genentech, support for attending meetings from Abbvie, Takeda and Janssen, and Participation on a Data Safety Monitoring Board or Advisory Board for AbbVie, AZ, Atlantic, Bristol-Myers Squibb, Galapagos, Janssen, Pfizer and Takeda. Prof. Lees reports a Future Leaders Fellow award from UKRI, personal consulting fees from Galapagos, Abbvie, Takeda, Pfizer, Janssen, Iterative Scopes and institutional consulting fees from Trellus Health, personal fees from Galapagos, Abbvie, Takeda, Pfizer, Janssen, GSK, Gilead, Fresenius Kabi, Ferring and Dr

Falk, and support for attending meetings from Galapagos, Abbvie, Takeda, Pfizer, Janssen, GSK, Gilead, Fresenius Kabi, Ferring and Dr Falk. Dr. Goodhand reports grants from F. Hoffmann-La Roche AG, grants from Biogen Inc, grants from Celltrion Healthcare, grants from Galapagos NV, non-financial support from Immundiagnostik, during the conduct of the study. Prof. Ahmad reports grant funding from Pfizer to his institution to deliver this study, grants from Celltrion, Roche, Takeda, Biogen and Galapagos and honoraria for lectures from Takeda and Roche, outside the submitted work. Dr Powell has received research grant(s) from Bristol Myers Squibb outside the submitted work. Dr. Powell reports personal fees from Takeda, Janssen, Pfizer, Bristol-Myers Squibb, Abbvie, Roche, Lilly, Allergan, and Celgene, outside the submitted work; Dr. Powell has served as a speaker/advisory board member for Abbvie, Allergan, Bristol Myers Squibb, Celgene, Falk, Ferring, Janssen, Pfizer, Tillotts, Takeda and Vifor Pharma. The following authors nothing to declare: Dr Ibraheim, Claire Bewshea, Rachel Nice, Dr Liu, Dr Mullish, Dr Danckert, Melissa Torkizadeh, Jesús Miguéns Blanco, Lauren A Roberts, Simeng Lin, Hemanth Prabhudev, Caroline Sands, Verena Horneffer-van der Sluis, Matthew Lewis, Professor Teare and Professor Marchesi.

## References

1. Lopez Bernal J, Andrews N, Gower C, et al. Effectiveness of the Pfizer-BioNTech and Oxford-AstraZeneca vaccines on covid-19 related symptoms, hospital admissions, and mortality in older adults in England: test negative case-control study. *BMJ (Clinical research ed)* 2021; **373**: n1088.
2. Andrews N, Tessier E, Stowe J, et al. Duration of Protection against Mild and Severe Disease by Covid-19 Vaccines. *The New England journal of medicine* 2022; **386**(4): 340–50.
3. Kennedy NA, Lin S, Goodhand JR, et al. Infliximab is associated with attenuated immunogenicity to BNT162b2 and ChAdOx1 nCoV-19 SARS-CoV-2 vaccines in patients with IBD. *Gut* 2021.
4. Alexander JL, Kennedy NA, Ibraheim H, et al. COVID-19 vaccine-induced antibody responses in immunosuppressed patients with inflammatory bowel disease (VIP): a multicentre, prospective, case-control study. *The lancet Gastroenterology & hepatology* 2022.
5. Lin S, Kennedy NA, Saifuddin A, et al. Antibody decay, T cell immunity and breakthrough infections following two SARS-CoV-2 vaccine doses in inflammatory bowel disease patients treated with infliximab and vedolizumab. *Nature communications* 2022; **13**(1): 1379.
6. Harris VC, Armah G, Fuentes S, et al. Significant Correlation Between the Infant Gut Microbiome and Rotavirus Vaccine Response in Rural Ghana. *The Journal of infectious diseases* 2017; **215**(1): 34–41.
7. Harris V, Ali A, Fuentes S, et al. Rotavirus vaccine response correlates with the infant gut microbiota composition in Pakistan. *Gut microbes* 2018; **9**(2): 93–101.
8. Hagan T, Cortese M, Roupael N, et al. Antibiotics-Driven Gut Microbiome Perturbation Alters Immunity to Vaccines in Humans. *Cell* 2019; **178**(6): 1313–28 e13.
9. Oh JZ, Ravindran R, Chassaing B, et al. TLR5-mediated sensing of gut microbiota is necessary for antibody responses to seasonal influenza vaccination. *Immunity* 2014; **41**(3): 478–92.

10. Lynn MA, Tumes DJ, Choo JM, et al. Early-Life Antibiotic-Driven Dysbiosis Leads to Dysregulated Vaccine Immune Responses in Mice. *Cell host & microbe* 2018; **23**(5): 653–60 e5.
11. Ng SC, Peng Y, Zhang L, et al. Gut microbiota composition is associated with SARS-CoV-2 vaccine immunogenicity and adverse events. *Gut* 2022.
12. Lloyd-Price J, Arze C, Ananthakrishnan AN, et al. Multi-omics of the gut microbial ecosystem in inflammatory bowel diseases. *Nature* 2019; **569**(7758): 655–62.
13. Franzosa EA, Sirota-Madi A, Avila-Pacheco J, et al. Gut microbiome structure and metabolic activity in inflammatory bowel disease. *Nature microbiology* 2019; **4**(2): 293–305.
14. Radhakrishnan ST, Alexander JL, Mullish BH, et al. Systematic review: the association between the gut microbiota and medical therapies in inflammatory bowel disease. *Alimentary pharmacology & therapeutics* 2022; **55**(1): 26–48.
15. Lee JWJ, Plichta D, Hogstrom L, et al. Multi-omics reveal microbial determinants impacting responses to biologic therapies in inflammatory bowel disease. *Cell host & microbe* 2021; **29**(8): 1294–304 e4.
16. Ding NS, McDonald JAK, Perdones-Montero A, et al. Metabonomics and the Gut Microbiome Associated With Primary Response to Anti-TNF Therapy in Crohn's Disease. *Journal of Crohn's & colitis* 2020; **14**(8): 1090–102.
17. Zhang X, Deeke SA, Ning Z, et al. Metaproteomics reveals associations between microbiome and intestinal extracellular vesicle proteins in pediatric inflammatory bowel disease. *Nature communications* 2018; **9**(1): 2873.
18. Devkota S, Wang Y, Musch MW, et al. Dietary-fat-induced taurocholic acid promotes pathobiont expansion and colitis in *Il10*<sup>-/-</sup> mice. *Nature* 2012; **487**(7405): 104–8.
19. Sahin U, Muik A, Vogler I, et al. BNT162b2 vaccine induces neutralizing antibodies and poly-specific T cells in humans. *Nature* 2021; **595**(7868): 572–7.
20. Skelly DT, Harding AC, Gilbert-Jaramillo J, et al. Two doses of SARS-CoV-2 vaccination induce robust immune responses to emerging SARS-CoV-2 variants of concern. *Nature communications* 2021; **12**(1): 5061.
21. Rath S, Heidrich B, Pieper DH, Vital M. Uncovering the trimethylamine-producing bacteria of the human gut microbiota. *Microbiome* 2017; **5**(1): 54.
22. Zhu W, Gregory JC, Org E, et al. Gut Microbial Metabolite TMAO Enhances Platelet Hyperreactivity and Thrombosis Risk. *Cell* 2016; **165**(1): 111–24.
23. Wang H, Rong X, Zhao G, et al. The microbial metabolite trimethylamine N-oxide promotes antitumor immunity in triple-negative breast cancer. *Cell Metab* 2022; **34**(4): 581–94 e8.
24. Jansson J, Willing B, Lucio M, et al. Metabolomics reveals metabolic biomarkers of Crohn's disease. *PloS one* 2009; **4**(7): e6386.
25. Bjerrum JT, Wang Y, Hao F, et al. Metabonomics of human fecal extracts characterize ulcerative colitis, Crohn's disease and healthy individuals. *Metabolomics: Official journal of the Metabolomic*

- Society 2015; **11**: 122–33.
26. Kolho KL, Pessia A, Jaakkola T, de Vos WM, Velagapudi V. Faecal and Serum Metabolomics in Paediatric Inflammatory Bowel Disease. *Journal of Crohn's & colitis* 2017; **11**(3): 321–34.
  27. Strazar M, Mourits VP, Koeken V, et al. The influence of the gut microbiome on BCG-induced trained immunity. *Genome biology* 2021; **22**(1): 275.
  28. Vernia P, Caprilli R, Latella G, Barbetti F, Magliocca FM, Cittadini M. Fecal lactate and ulcerative colitis. *Gastroenterology* 1988; **95**(6): 1564–8.
  29. Hallert C, Bjorck I, Nyman M, Pousette A, Granno C, Svensson H. Increasing fecal butyrate in ulcerative colitis patients by diet: controlled pilot study. *Inflammatory bowel diseases* 2003; **9**(2): 116–21.
  30. Ortiz-Masia D, Gisbert-Ferrandiz L, Bauset C, et al. Succinate Activates EMT in Intestinal Epithelial Cells through SUCNR1: A Novel Protagonist in Fistula Development. *Cells* 2020; **9**(5).
  31. Banerjee A, Herring CA, Chen B, et al. Succinate Produced by Intestinal Microbes Promotes Specification of Tuft Cells to Suppress Ileal Inflammation. *Gastroenterology* 2020; **159**(6): 2101–15 e5.
  32. Muench P, Jochum S, Wenderoth V, et al. Development and Validation of the Elecsys Anti-SARS-CoV-2 Immunoassay as a Highly Specific Tool for Determining Past Exposure to SARS-CoV-2. *Journal of clinical microbiology* 2020; **58**(10).
  33. Amplicon P, Clean-Up P, Index P. 16s metagenomic sequencing library preparation. *Illumina com* 2013.
  34. Mullish BH, Pechlivanis A, Barker GF, Thursz MR, Marchesi JR, McDonald JAK. Functional microbiomics: Evaluation of gut microbiota-bile acid metabolism interactions in health and disease. *Methods* 2018; **149**: 49–58.
  35. Callahan BJ, McMurdie PJ, Rosen MJ, Han AW, Johnson AJ, Holmes SP. DADA2: High-resolution sample inference from Illumina amplicon data. *Nat Methods* 2016; **13**(7): 581–3.
  36. Davis NM, Proctor DM, Holmes SP, Relman DA, Callahan BJ. Simple statistical identification and removal of contaminant sequences in marker-gene and metagenomics data. *Microbiome* 2018; **6**(1): 226.
  37. Liu Z, Xia B, Saric J, et al. Effects of Vancomycin and Ciprofloxacin on the NMRI Mouse Metabolism. *Journal of proteome research* 2018; **17**(10): 3565–73.
  38. Veselkov KA, Lindon JC, Ebbels TM, et al. Recursive segment-wise peak alignment of biological (1)h NMR spectra for improved metabolic biomarker recovery. *Analytical chemistry* 2009; **81**(1): 56–66.
  39. Dieterle F, Ross A, Schlotterbeck G, Senn H. Probabilistic quotient normalization as robust method to account for dilution of complex biological mixtures. Application in 1H NMR metabolomics. *Analytical chemistry* 2006; **78**(13): 4281–90.
  40. Cloarec O, Dumas ME, Craig A, et al. Statistical total correlation spectroscopy: an exploratory approach for latent biomarker identification from metabolic 1H NMR data sets. *Analytical chemistry*

- 2005; **77**(5): 1282–9.
41. Sarafian MH, Lewis MR, Pechlivanis A, et al. Bile acid profiling and quantification in biofluids using ultra-performance liquid chromatography tandem mass spectrometry. *Analytical chemistry* 2015; **87**(19): 9662–70.
  42. Mullish BH, McDonald JAK, Pechlivanis A, et al. Microbial bile salt hydrolases mediate the efficacy of faecal microbiota transplant in the treatment of recurrent *Clostridioides difficile* infection. *Gut* 2019; **68**(10): 1791–800.
  43. Lewis MR, Pearce JT, Spagou K, et al. Development and Application of Ultra-Performance Liquid Chromatography-TOF MS for Precision Large Scale Urinary Metabolic Phenotyping. *Analytical chemistry* 2016; **88**(18): 9004–13.
  44. Wolfer AM, Correia GDS, Sands CJ, et al. peakPantheR, an R package for large-scale targeted extraction and integration of annotated metabolic features in LC-MS profiling datasets. *Bioinformatics (Oxford, England)* 2021.
  45. Sands CJ, Wolfer AM, Correia GDS, et al. The nPYc-Toolbox, a Python module for the pre-processing, quality-control and analysis of metabolic profiling datasets. *Bioinformatics (Oxford, England)* 2019; **35**(24): 5359–60.
  46. McMurdie PJ, Holmes S. phyloseq: an R package for reproducible interactive analysis and graphics of microbiome census data. *PLoS One* 2013; **8**(4): e61217.
  47. Oksanen J, Guillaume Blanchet F, Friendly M, et al. Package ‘vegan’. 2020. <https://cran.r-project.org>, <https://github.com/vegandevs/vegan> (accessed 26/07/2021 2021).
  48. Wickham H. *ggplot2 Elegant Graphics for Data Analysis*. Second ed: Springer Nature; 2016.
  49. Bates D, Machler M, Bolker BM, Walker SC. Fitting Linear Mixed-Effects Models Using lme4. *J Stat Softw* 2015; **67**(1): 1–48.
  50. Aitchison J. The Statistical Analysis of Compositional Data. *Journal of the Royal Statistical Society: Series B (Methodological)* 1982; **44**(2): 139–60.
  51. Gloor GB, Macklaim JM, Pawlowsky-Glahn V, Egozcue JJ. Microbiome Datasets Are Compositional: And This Is Not Optional. *Front Microbiol* 2017; **8**: 2224.
  52. Lin H, Peddada SD. Analysis of compositions of microbiomes with bias correction. *Nature communications* 2020; **11**(1): 3514.
  53. Martinez-Gili L, McDonald JAK, Liu Z, et al. Understanding the mechanisms of efficacy of fecal microbiota transplant in treating recurrent *Clostridioides difficile* infection and beyond: the contribution of gut microbial-derived metabolites. *Gut microbes* 2020; **12**(1): 1810531.

## Supplementary Figure

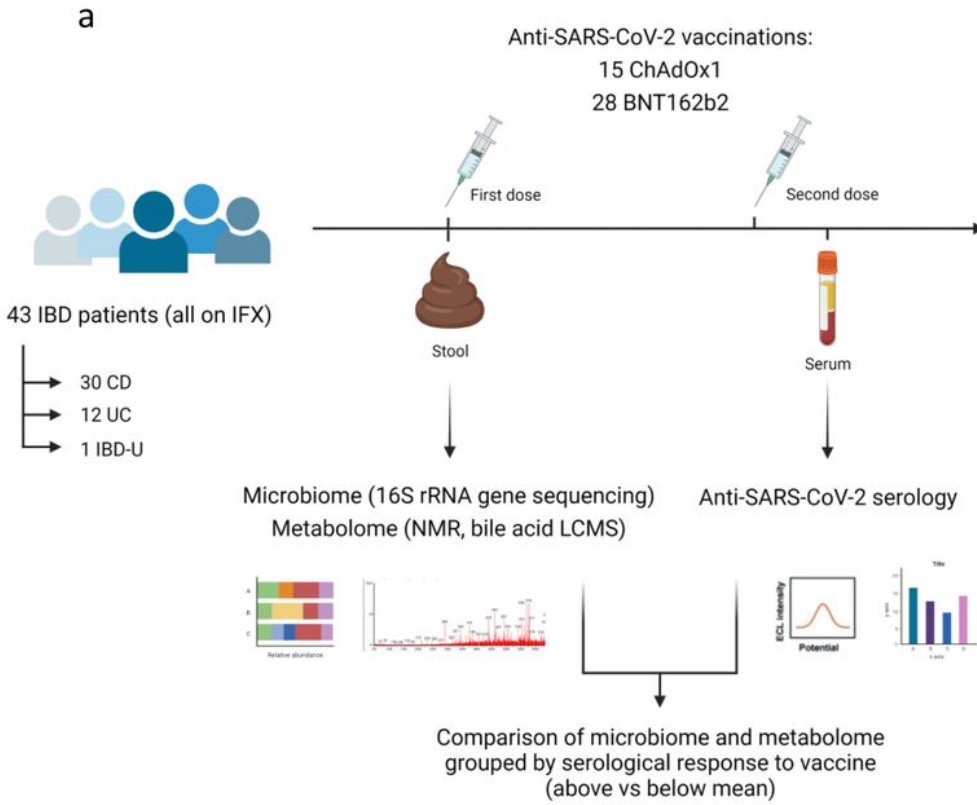
Supplementary Figure 1 is not available with this version.

### Supplementary figure legend:

(a) Age distribution of participants with above (left) and below (right) average vaccine responses. The horizontal lines signify the median age in each group. (b) IBD subtype, (c) gender, (d) vaccine type and (e) use of immunomodulator distribution in above and below average vaccine responders. P values calculated using Mann-Witney test for continuous variables and Fisher's exact test for categorical variables.

## Figures

**Figure 1**



**b**

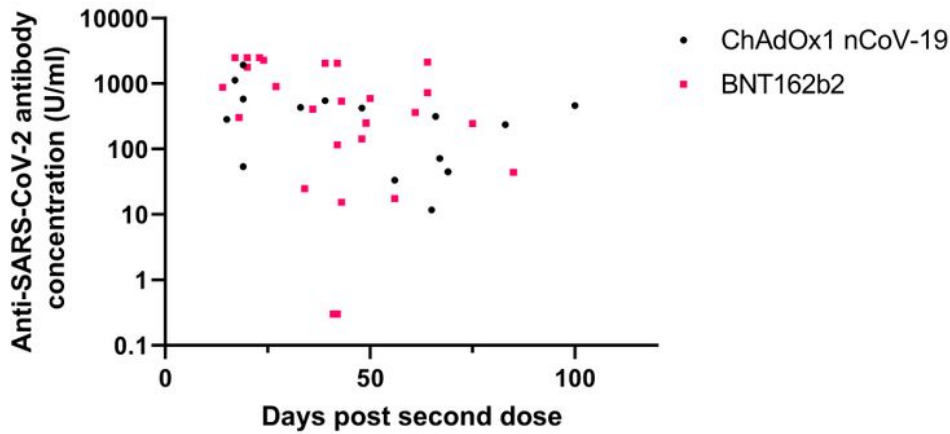


**Figure 1**

(a) Experimental schema for the study; (b) Anti-SARS-CoV-2 spike RBD antibody concentrations in patients receiving ChAdOx1 nCoV-19 (black dots) or BNT162b2 (pink squares). Each point represents a single patient plotted the number of days after second dose of vaccine when their antibody level was measured

**Figure 2**

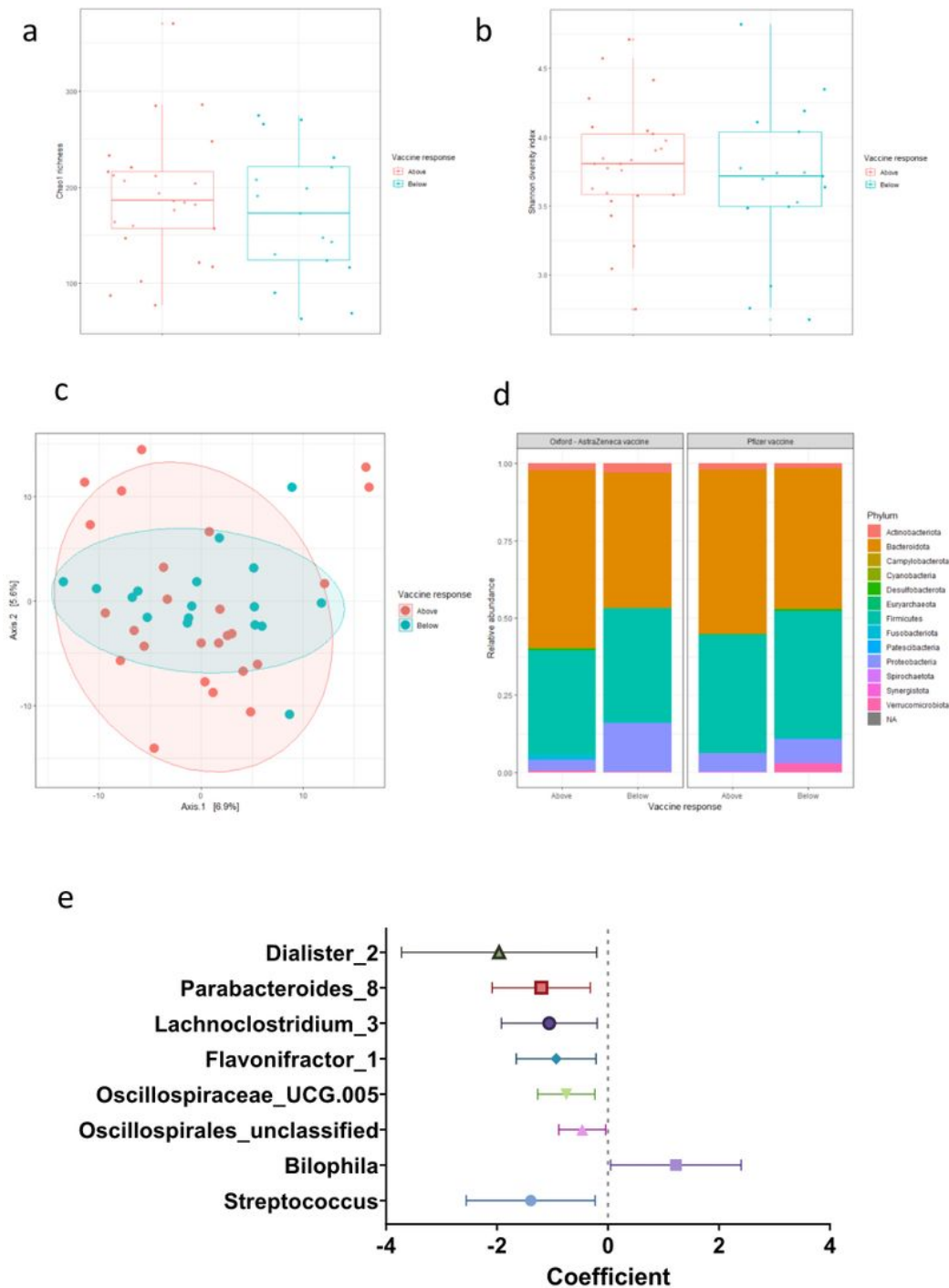


**Figure 2**

**Gut microbiota composition associated with serological response to two doses of anti-SARS-CoV-2 vaccine.** (a) Chao1 and (b) Shannon Diversity metrics, showing no difference in alpha diversity between above (red) and below (blue) average vaccine responders (Kruskal-Wallis tests  $p=ns$ ); (c) Principal coordinates analysis (PCoA) plot of Aitchison's distances in above (red) and below (blue) average responders (numbers on points represent study number; Permutation Test for Constrained

Correspondence Analysis, Redundancy Analysis and Constrained Analysis of Principal Coordinates  $p=0.021$ ; PERMANOVA test  $p=ns$ ); (d) Phylum level relative abundance bar plots for above and below average responders to Oxford/Astra-Zeneca (ChadOx-nCoV-19) vaccine (left) and Pfizer/BioNTech (BNT162b2) vaccine (right). (e) Univariate analysis of ASVs identified as differentially abundant between above and below average vaccine responders.

**Figure 3**

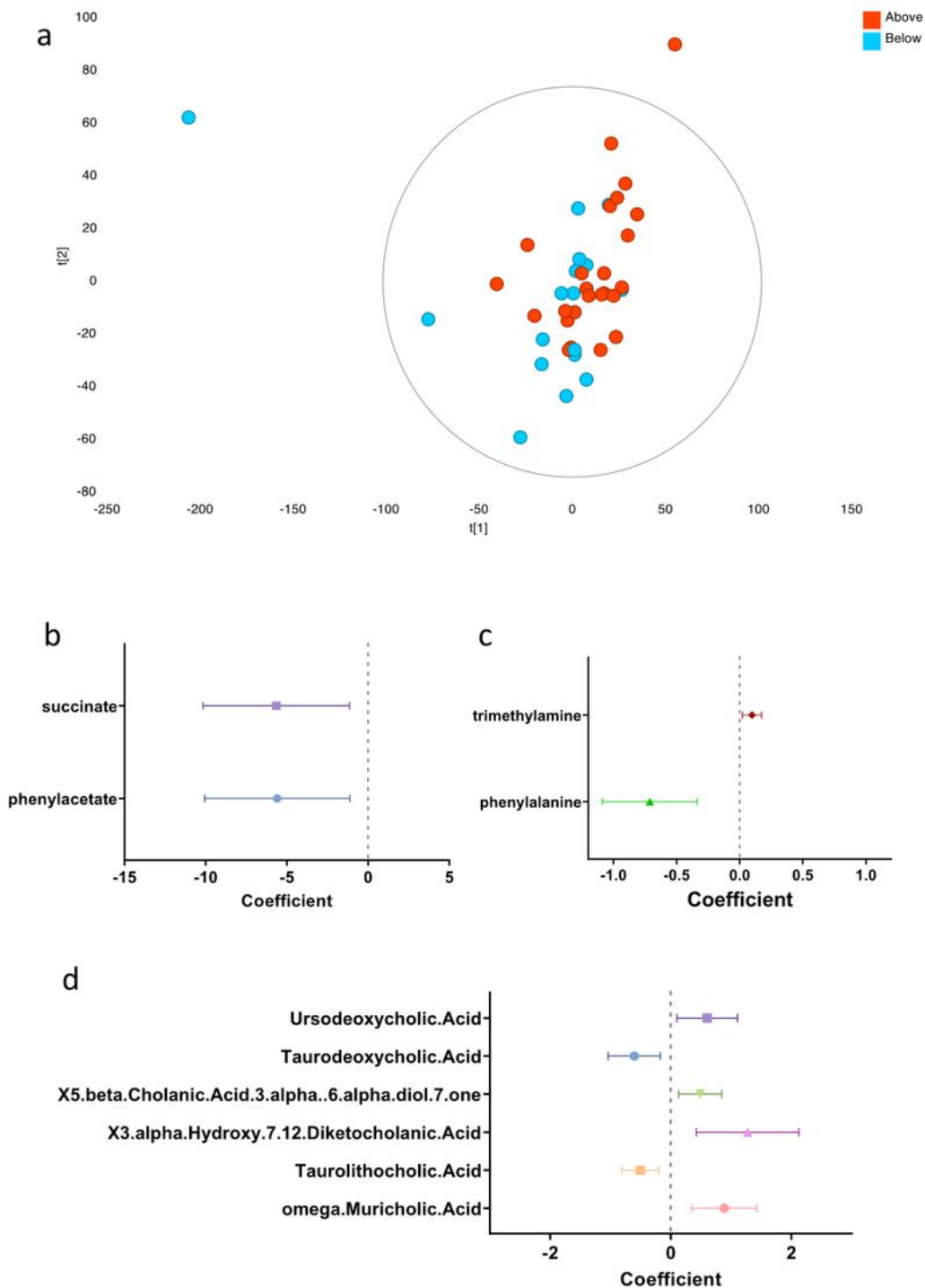


**Figure 3**

**Faecal metabolomics show associations between gut microbial function and serological response to vaccination.** (a) Principal Components Analysis showing clustering of participants based on 1H-NMR profile (2 PCs,  $R^2 = 0.42$ ,  $Q^2 0.12$ ; OPLS-DA model (not shown)  $R^2X 0.25$ ,  $R^2Y 0.26$ ,  $Q^2 0.15$ ; CV-ANOVA  $p=0.038$ ). (b) & (c) Univariate analysis of metabolites identified as differentially abundant between above and below average vaccine responders in 1H-NMR. (d) Univariate analysis of bile acids identified as differentially abundant between above and below average vaccine responders in UPLC-MS.

**Figure 4**

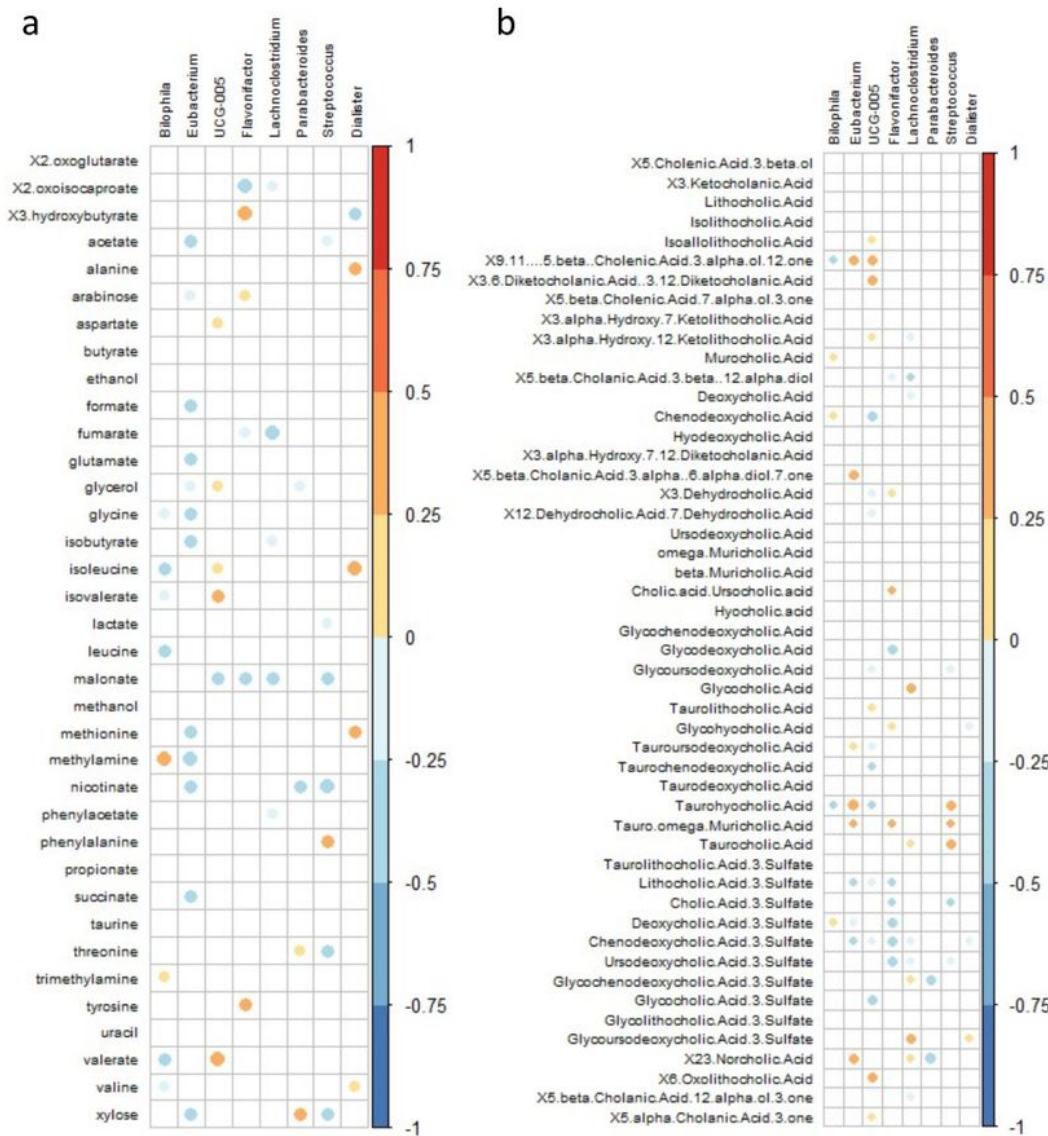


## Figure 4

**Spearman correlation heatmaps showing associations between gut microbiota and metabolites.** ASVs shown were identified as associated with above/below average response to vaccination and correlated with (a) metabolites identified from <sup>1</sup>H-NMR and (b) bile acids. Coloured circles signify correlations with q value <0.2.